



OPEN ACCESS

EDITED BY

Alejandro Parola,
National University of Quilmes, Argentina

REVIEWED BY

Christina Marie Lisk,
University of Colorado Anschutz Medical
Campus, United States
María Inés Becker,
Science and Technology for Development
Foundation (Fucited), Chile

*CORRESPONDENCE

Marcos Sebastián Dreon
✉ msdreon@med.unlp.edu.ar

RECEIVED 02 September 2024

ACCEPTED 16 December 2024

PUBLISHED 08 January 2025

CITATION

Chiumiento IR, Tricerri MA, Cortéz MF,
Ituarte S, Tau J, Mariño KV, Smaldini PL,
Heras H and Dreon MS (2025) *Pomacea
canaliculata* hemocyanin as a novel natural
immunostimulant in mammals.
Front. Immunol. 15:1490260.
doi: 10.3389/fimmu.2024.1490260

COPYRIGHT

© 2025 Chiumiento, Tricerri, Cortéz, Ituarte,
Tau, Mariño, Smaldini, Heras and Dreon. This is
an open-access article distributed under the
terms of the [Creative Commons Attribution
License \(CC BY\)](#). The use, distribution or
reproduction in other forums is permitted,
provided the original author(s) and the
copyright owner(s) are credited and that the
original publication in this journal is cited, in
accordance with accepted academic
practice. No use, distribution or reproduction
is permitted which does not comply with
these terms.

Pomacea canaliculata hemocyanin as a novel natural immunostimulant in mammals

Ignacio Rafael Chiumiento^{1,2}, María Alejandra Tricerri^{1,3},
María Fernanda Cortéz¹, Santiago Ituarte^{1,4}, Julia Tau¹,
Karina Valeria Mariño⁵, Paola Lorena Smaldini⁶, Horacio Heras^{1,2}
and Marcos Sebastián Dreon^{1,4*}

¹Instituto de Investigaciones Bioquímicas de La Plata "Prof. Dr. Rodolfo R. Brenner", (INIBIOLP),
Universidad Nacional de La Plata (UNLP) - Consejo Nacional de Investigaciones Científicas y Técnicas
(CONICET), La Plata, Argentina, ²Cátedra de Química Biológica, Facultad de Ciencias Naturales y
Museo, UNLP, La Plata, Argentina, ³Cátedra de Bioquímica Clínica I, Facultad de Ciencias Médicas,
UNLP, La Plata, Argentina, ⁴Cátedra de Bioquímica y Biología Molecular, Facultad de Ciencias
Médicas, UNLP, La Plata, Argentina, ⁵Laboratorio de Glicómica Funcional y Molecular, Instituto de
Biología y Medicina Experimental (IBYME), CONICET, Buenos Aires, Argentina, ⁶Instituto de Estudios
Inmunológicos y Fisiopatológicos (IIFP), UNLP - CONICET, La Plata, Argentina

Introduction: Gastropod hemocyanins are potent immunostimulants in mammals, a trait associated with their large molecular size and unusual glycosylation patterns. While the hemocyanin from the marine snail keyhole limpet (KLH), has been widely studied and successfully employed as a carrier/adjuvant in several immunological applications, as well as a non-specific immunostimulant for bladder cancer treatment, few other gastropod hemocyanins have been biochemically and immunologically characterized. In this work, we investigated the immunogenic properties of the hemocyanin from *Pomacea canaliculata* (PcH), an invasive south American freshwater snail. This species, known for its high reproductive rate and easy rearing, represents a promising source of potential biomedical compounds, including hemocyanin.

Methods: Employing flow cytometry, fluorescence microscopy, immunoassays, and quantitative PCR, we analysed the effects of PcH on THP-1 monocytes and their derived macrophages, as well as its ability to induce humoral response on C57BL/6 mice. Additionally, we evaluated the structural stability of PcH across a wide range of temperature and pH values.

Results and discussion: Our findings demonstrate that PcH is a structurally stable protein that not only triggers a pro-inflammatory effect on THP-1 derived-macrophages by increasing IL1- β and TNF- α levels, but also promotes phenotypic changes associated with the monocyte-to-macrophage differentiation. Moreover, the humoral response induced by PcH in mice was indistinguishable from that of KLH, highlighting the promising immunostimulatory properties of this freshwater snail hemocyanin.

KEYWORDS

gastropods, mollusc, respiratory pigment, innate immunity, macrophage

1 Introduction

Molluscan hemocyanins are large respiratory proteins widely distributed among invertebrates in nature. They are enormous multimeric glycoproteins freely dissolved in the haemolymph, representing up to 90% of the total protein content in this fluid (1). Structurally, these respiratory proteins consist of partially hollow cylinders, composed of ten subunits, each around 400 kDa, associated in di-, tri-, and even multi-decamers. Thus, they are among the largest proteins in nature, with molecular masses ranging from 4 to 8 MDa or even higher. In addition, they exhibit high thermal stability, with melting temperature reaching up to 80°C in some species (2–4). Despite these common structural features, the great mollusc diversity leads to marked differences among groups (5).

In the last decades, immunotherapies have emerged as alternatives to traditional chemotherapies, particularly in developing new antitumoral treatments (6, 7). Notably, molluscan hemocyanins are potent natural immunostimulants in mammals, enhancing both innate and adaptive immune responses with promising clinical outcomes (8, 9). They have been used as carrier proteins coupled to different antigens, including tumour-associated carbohydrate antigens (TACA) (10, 11). They also serve as non-specific immunostimulants in therapeutic cancer vaccines and other anti-tumour strategies, acting as adjuvants to counteract immune self-tolerance to tumour antigens (8, 12). The immunomodulatory effects of hemocyanins are linked to their unique features such as their enormous size which allows for prolonged antigen presentation (8), and their heterogeneous glycosylation patterns (13, 14). These patterns include methylated hexoses, fucose or xylose residues, and truncated N-glycans (14, 15). These glycans interact with immune receptors like C-type lectin receptors and Toll-like receptor 4 on leukocytes, promoting the secretion of Th1-type inflammatory cytokines (16).

The first molluscan hemocyanin employed in biomedical studies was the keyhole limpet hemocyanin (KLH), isolated from the haemolymph of the marine gastropod *Megathura crenulata* (9). KLH has been successfully employed as a non-specific immunostimulant for the treatment of recurrent superficial bladder cancer, with negligible toxic side effects (17), making it an ideal therapeutic agent for long-term continuous treatment. In the last decades, due to the limited bioavailability and growing demand for KLH, there has been a marked interest in identifying and characterizing new hemocyanins with similar or better immunological properties. In this sense, various new gastropod hemocyanins have been studied, mostly from marine species such as RtH from *Rapana thomasiana* (18–20), HtH from *Haliotis tuberculata* (21, 22), CCH from *Concholepas concholepas* (23, 24), FLH from *Fissurella latimarginata* (25), and HaH from the pulmonated *Helix aspersa* (20).

Recently, a hemocyanin was isolated from a freshwater snail, *Pomacea canaliculata* (Caenogastropoda, Ampullariidae). This protein named PcH is a KLH-type hemocyanin organized in decamers of 390 kDa subunits (26). The glycan moiety of PcH (2.8% w/w) includes terminal galactose and GalNAc residues, as well as high mannose and complex type N-glycans, containing structures compatible with the T-antigen (27). PcH is of particular interest

because it can be purified in large quantities from adult *P. canaliculata*, a South American freshwater snail. This species is especially significant as it is an invasive species with a high reproductive potential and is easy to rear in laboratory conditions. Since its introduction to China in the 1980s, it has rapidly spread worldwide, prompting extensive studies on its biology, physiology, and metabolism (28). These attributes highlight the potential of this species as a source of compounds with promising biomedical use, such as PcH.

In the present work, we study the immunostimulant properties of PcH and evaluate its structural stability to explore its potential application as a bioactive compound. We evaluated the effect of PcH on macrophages focusing on pro-inflammatory cytokines, and the morphophysiological changes induced in a human monocyte leukemic cell line employing flow cytometry, fluorescence microscopy, immunoassays, and quantitative PCR. In addition, we evaluated *in vivo* the immunogenic activity of PcH in C57BL/6 mice measuring the sera IgG titers by ELISA and characterized its structural stability against temperature and extreme pH values by absorption and fluorescence spectroscopy.

2 Materials and methods

2.1 Animals

Adult *P. canaliculata* snails were collected in water streams near La Plata city, Buenos Aires province, Argentina (40° 42' 46'' S, 74° 0' 21'' W), genetically identified by sequencing a cytochrome C oxidase I gene fragment by using LCO1490 and HCO2198 primers (29), and reared in the laboratory. All studies followed the legislation of the Argentinean provincial Wildlife Hunting Law (Ley 5786, Art. 2).

Six-week-old female C57BL/6JLAE mice were obtained from the Experimental Animals Laboratory of the School of Veterinary Science (UNLP, Argentina), housed in the facilities of the School of Medicine (UNLP, Argentina), at 22°C with light/dark cycle of 12/12 h and fed *ad libitum* with sterile food and water.

Studies complied with the Guide for the Care and Use of Laboratory Animals (30) and were approved by the “Comité Institucional de Cuidado y Uso de Animales de Experimentación” (CICUAL) of the School of Medicine, UNLP (P02-01-2024).

2.2 Protein sample preparation, NaIO₄ treatment, and de-N-glycosylation

Lyophilized KLH was purchased from Sigma Chemical Co. (Cat. No. H7017), reconstituted in phosphate buffer saline (PBS) according to the manufacturer’s guidelines and sterilized by 0.22 μm filtration. Native PcH was isolated from the haemolymph collected through exsanguination of 6 adult snails under sterile and pyrogen-free conditions. The purification of PcH was performed as previously described (27). Briefly, samples were pooled, and cell free haemolymph was obtained by sequential centrifugation at 500 x g, 10 min and 10,000 x g, 10 min. The

obtained supernatant was layered on a tube containing NaBr ($\delta = 1.28 \text{ g/mL}$) and centrifuged at $200,000 \times g$, 22 h, in a swinging bucket rotor SW60.Ti on a Beckman L8M (Beckman, Palo Alto, CA). After centrifugation, PcH-containing fractions -blue color bands- were collected and pooled to further purify the protein by size exclusion liquid chromatography on a Superose-6 column (Amersham-Pharmacia, Uppsala, Sweden) coupled to an Agilent 1260 HPLC system (Agilent Technologies) using two different mobile phases, PBS or 20 mM Tris-HCl pH 7.4, 20 mM CaCl_2 and MgCl_2 buffer, as appropriate for the experiments. Deglycosylated PcH forms were obtained by an oxidative procedure incubating with 15 mM sodium periodate for 1 h in the dark at room temperature as previously described (31). PcH was also de-N-glycosylated by treatment with glycerol-free PNGase F (New England Biolabs) using dissociating conditions to give better access to oligosaccharides, as previously described by Salazar and coworkers (32). Briefly, PcH was dialyzed against dissociation buffer (130 mM glycine containing 2.5 mM EDTA, pH 8.6), and then heated at 60 or 100°C for 15 min. PcH was then cooled to room temperature, and 2 μL of PNGase F in deionized water was added and incubated for 24 h at 37°C. After deglycosylation, both PcH samples were washed with PBS and concentrated to 1 mg/mL employing an Amicon Ultra-15 50K MWCO device (Millipore). Glycan removal was verified through PAGE analysis, by comparing the electrophoretic pattern of the deglycosylated PcH forms with the negative control for each treatment. The protein content of PcH preparations was determined spectrophotometrically at 280 nm and their purity was checked using PAGE. For cell culture assays, hemocyanin samples were sterilized by filtration through 0.22 μm membranes and endotoxin levels were determined spectrophotometrically, following the method described by Karkhanis and coworkers (33).

2.3 PcH structural stability against pH and temperature

To evaluate the influence of pH on the protein structure, 1.0 mg/mL PcH at pH values ranging from 2.0 to 12.0 were prepared. Buffers were formulated using 100 mM sodium phosphate salts, except for pH 4.0 buffer which was prepared by mixing 100 mM sodium citrate and 200 mM Na_2HPO_4 0.2 M. Samples were incubated for 48 h at 4°C in the dark and analysed by fluorescence and absorption spectroscopy at 25°C.

To assess thermal stability, 0.6 g/L PcH dissolved in 20 mM Tris-HCl buffer (pH 7.4) containing 10 mM CaCl_2 and 10 mM MgCl_2 was subjected to rising temperatures from 25 to 85°C. Once the desired temperature was stable, fluorescence and absorption spectra were acquired.

2.3.1 Absorption spectroscopy

UV-visible spectra were recorded between 250 and 310 nm using an Agilent 8453 diode array spectrophotometer (Agilent Technologies, Waldbronn, Germany). The temperature of the sample holder was controlled using a circulating water bath

(Lauda-Königshofen, Germany). For each sample, three spectra were acquired and averaged, and its corresponding buffer was subtracted. In all cases, the fourth derivative spectra were calculated.

2.3.2 Fluorescence spectroscopy

Intrinsic fluorescence spectra of PcH at different temperatures and pH values were recorded in emission scanning mode in a Varian Cary Eclipse spectrofluorometer (Varian Inc., Australia). Tryptophan residues were excited at 290 nm (5 nm slit) and the emission was recorded between 310 and 410 nm (5 nm slit) in a 1 cm optical path quartz-cell. The temperature of the sample holder was controlled by employing a circulating water bath (LAUDA, Lauda-Königshofen, Germany). For each sample, three emission spectra were acquired, averaged, and corrected for buffer fluorescence. In all cases, the mass center was calculated.

2.4 Cell culture

The human pro-monocyte cell line THP-1 was obtained from ECACC (Salisbury, UK). Cells were cultured in RPMI 1640 medium (Serendipia Lab, Buenos Aires, Argentina) with 25 mM sodium bicarbonate, 25 mM HEPES, pH 7.3 supplemented with 10% v/v fetal bovine serum (FBS, NATOCOR, Villa Carlos Paz, Córdoba, Argentina), and 100 nM penicillin/streptomycin (Life Technologies, Grand Island, NY) at 37°C with 5% CO_2 in a humidified atmosphere. The cellular density was kept below $5 \times 10^5/\text{mL}$ by diluting the cultures with fresh medium every 5 to 7 days.

2.4.1 Pro-inflammatory effects of PcH

To promote macrophage transformation, THP-1 cells were seeded on a 24-well plate at approximately 10^6 cells/mL (0.5×10^6 cells/well), and exposed to 5 ng/mL phorbol 12-myristate 13-acetate (PMA, Sigma Chemical Co.), for 48 h. Once transformed, the PMA-containing medium was removed, and the macrophages were washed twice with PBS and cultured for 24 h in fresh medium. Finally, cells were exposed for 3 h to PcH as well as to its deglycosylated forms, at concentrations ranging from 0.015 to 1.000 g/L in PBS, employing 50 ng/mL of lipopolysaccharide (LPS, Sigma Chemical Co.) and PBS as positive and negative control of the assay, respectively. After treatments, cell viability was evaluated by 3-[4,5-dimethylthiazol-2-yl]-2,5-diphenyltetrazolium bromide (MTT, Sigma Chemical Co.) assay as we previously described (34) and the levels of TNF- α and interleukin-1 β were determined in the culture supernatants by ELISA (BD Biosciences, San Diego, CA) as previously described (35).

2.4.2 Effect of PcH on monocyte differentiation

To evaluate the ability of PcH to promote THP-1 cell differentiation to macrophages, THP-1 cells were seeded on multiwell plates at approximately 10^6 cells/mL unless otherwise stated and incubated with 1 g/L of the purified protein in PBS buffer. The phenotypic changes observed were measured and compared with 5 ng/mL of PMA and PBS as positive and negative controls,

respectively. Experiments were performed by triplicates and cell morphology, cell adhesion, and gene differential expression of different macrophage markers were analysed as described below.

2.4.2.1 Cell adhesion

Cell adhesion was evaluated employing the Hoescht-33258 fluorophore. Briefly, cells were seeded on 96-multiwell plates and incubated for 24 h either in the presence or absence of PcH, as described above. Culture supernatants were centrifugated at 500 x g, 10 min and the pelleted cells were washed with RPMI 0.5% FBS, the obtained pellet was resuspended in distilled water and incubated for 15 min in the dark at 37°C with 100 µL of Hoescht-33258 (Sigma Chemical Co.), 0.02 mg/mL in TNE buffer (Tris-HCl 10 mM, pH=7.4, NaCl 2 M, EDTA 1 mM). Well-adhered cells were treated similarly. Sample fluorescence was registered at 460 nm (λ_{ex} , 358 nm) in a multiwell reader DTX 880 (Beckman Coulter, CA, USA). In addition, images of adhered and non-adhered cells were acquired in an inverted fluorescence microscope (Olympus IX-71, Tokyo, Japan).

2.4.2.2 Flow cytometry

THP-1 monocyte cells were seeded in a multi-12 well plate and incubated for 72 h in RPMI 0.5% FBS with PcH 1 mg/mL, PBS or PMA 5 ng/mL. The culture supernatant, containing the non-adhered cells, was taken and the adhered cells were gently scrapped and resuspended in fresh medium. Both cell populations of each treatment were pooled, washed once, and resuspended in PBS, and their cell size and granularity were inferred by the forward (FSC) and side scattered (SSC) light respectively. Additionally, to further evaluate this differentiation process, the same experiment was performed and, before harvesting, cells were incubated for 15 min at 37°C with 1 nM MitoTracker DeepRed (Invitrogen, Waltham, MA, USA), a mitochondrial-potential dependent dye, dissolved in RPMI without neither phenol red nor FBS.

The assays were performed on a BD Accuri™ C6 Plus Flow Cytometer (BD Bioscience, San Diego, CA, USA), with a two-laser base configuration: 488 nm solid-state blue laser and 640 nm diode red laser, carrying standard optical filters: FL1 533/30 nm, FL2 585/40 nm, FL3 >670 nm and FL4 675/25 nm. The latter was employed

for detecting the emission of MitoTracker DeepRed excited by the 640 nm laser. Cells solely incubated with RPMI were employed as autofluorescence control and subtracted to the median fluorescence intensity (MdfI) of each treatment. For each sample 50,000 events were recorded.

Data transformation and analysis were performed using the FlowJo™ X 10.0.7r2 Software (BD Life Sciences). To define populations, the FSC-A vs SSC-A gate was used for all data files. Experiments were performed by triplicates or quadruplicates.

2.4.2.3 Quantitative RT-PCR

THP-1 cells were seeded in 60 mm culture plates at a density of 2.5×10^6 cells/mL (2.5×10^6 cells/plate) and cultured for 36 h in the presence of 1 g/L of PcH and 5 ng/mL of PMA. Total RNA was isolated from cultures using TRIzol reagent (Thermo Fisher Scientific Inc.) following the manufacturer's instructions. The absence of genomic DNA as well as RNA integrity was checked in a 1% agarose gel electrophoresis and total RNA content was quantified at 260 nm in a Nanodrop 2000/2000c (Thermo Fisher Scientific Inc.). Synthesis of cDNA was performed using the iScript cDNA Synthesis Kit (BIO-RAD Laboratories, Inc., Hercules, CA, USA) following the manufacturer's instructions. Real-time PCR was performed in a AriaMix (Agilent Technologies, Inc) thermocycler using a qPCR iTaq Universal SYBR Green Supermix, (BIO-RAD Laboratories, Inc., Hercules, CA, USA) to determine the relative gene expression levels in each sample employing the following quantitation formula:

$$\text{Ratio} = \frac{(E_{\text{TARGET}})^{\Delta Cq_{\text{TARGET}}(\text{CALIBRATOR}-\text{SAMPLE})}}{(E_{\text{REFERENCE}})^{\Delta Cq_{\text{REFERENCE}}(\text{CALIBRATOR}-\text{SAMPLE})}}$$

where E is the qPCR efficiency for each gene, calculated in the corresponding calibration curves as $10^{(1-\text{SLOPE REGRESSION LINE})-1}$, $TARGET$ means each of the markers which expression was evaluated, $REFERENCE$ is the housekeeping gene employed, *i.e.* GAPDH, and $CALIBRATOR$ the PBS-treated cells used as negative control.

The oligonucleotide primer sequences for well-characterized macrophage markers, including CD-80, CD-86, iNOS, CD-206, CD-263, and CD-11b, as well as GAPDH used as housekeeping gene, are listed in Table 1.

TABLE 1 Oligonucleotide primer sequences employed to evaluate the differential expression of macrophage markers.

	GENE	FORWARD PRIMER	REVERSE PRIMER
Pan Macrophage	CD68	CGAGCATCATTCTTTCACCAGCT	ATGAGAGGCAGCAAGATGGACC
	CD11b	GGAACGCCATTGTCTGCTTTTCG	ATGCTGAGGTCATCCTGGCAGA
M1	CD86	CCATCAGCTGTGCTGTTTCATTCC	GCTGTAATCCAAGGAATGTGGTC
	CD80	CTCTTGGTGCTGGCTGGTCTTT	GCCAGTAGATGCGAGTTTGTGC
	iNOS	GCTCTACACCTCCAATGTGACC	CTGCCGAGATTTGAGCCTCATG
M2	CD163	CCAGAAGGAACCTGTAGCCACAG	CAGGCACCAAGCGTTTTGAGCT
	CD206	AGCCAACACCAGCTCCTCAAGA	CAAAACGCTCGCGCATTGTCCA
Reference	GAPDH	GAGTCAACGGATTTGGTCGT	TTGATTTTGGAGGGATCTCG

2.4.2.4 Quantitation of CD-68 by Western blot

THP-1 cells were seeded in 12-well plates and incubated with 1 g/L of purified PcH in PBS for 72 h. Negative and positive controls were obtained by incubating cells with PBS and 5 ng/mL PMA, respectively. Plates were centrifugated at 500 x g for 10 min, the supernatant discarded, and the cell culture total proteins extracted with 40 μ L of RIPA lysis buffer and quantified by Bradford (36). Then, 5 μ g of each protein sample was resolved in a 4-12% SDS-PAGE gel and transferred onto a nitrocellulose membrane at 100 V for 1 h in a Transblot Cell (Bio Rad Laboratories, Inc.), using 25 mM Tris-HCl, 192 mM glycine, 20% (v/v) methanol, pH 8.5 buffer. After transfer, membrane was blocked with 5% (w/v) non-fat dry milk in PBS-Tween 0.05% (v/v) for 1 h, and then incubated overnight at 4°C with an anti-CD68 mouse monoclonal antibody diluted 1/10,000 in 1% (w/v) non-fat dry milk in PBS-Tween. After washing with PBS-Tween, the membrane was incubated with goat anti-mouse IgG horseradish peroxidase conjugate (BioRad Laboratories, Inc.) diluted 1/20,000. Immunoreactivity was visualized by ECL in a ChemiDoc Imaging System (BioRad Laboratories, Inc.).

2.5 Humoral immunity bioassays

To evaluate the immunogenicity of PcH *in vivo*, groups of three mice were inoculated intraperitoneally with 100 μ L of either KLH (Sigma-Aldrich) or PcH, both at 2 g/L in PBS. A third group received the same volume of PBS. Fifteen days later, the immunization was repeated, and ten days after that, mice were euthanized by cervical dislocation and bled by cardiac puncture.

The specific anti-PcH IgG levels in the sera were determined by ELISA. Briefly, 96-well plates (NUNC MaxiSorp, Thermo Scientific) were coated with 100 μ L/well at 25 μ g/mL of either PcH or KLH in carbonate buffer (pH 9.6) overnight at 4°C. The plates were then washed three times with PBS-Tween 0.05% (v/v) and blocked with 200 μ L/well of 3% (w/v) non-fat dry milk in PBS for 1 h at 37°C. After blocking, plates were incubated with 100 μ L/well of two-fold serial dilutions of the obtained sera in PBS, 1% (w/v) non-fat dry milk, for 1 h at 37°C. Then, plates were washed and incubated with anti-mouse IgG HRP (BioRad Laboratories, Inc.) (1/10,000 dilution in 1% w/v non-fat dry milk in PBS) 1 h at 37°C. Finally, the plates were washed again and developed by adding 100 μ L/well of 1 mg/mL o-phenylenediamine dihydrochloride (OPD) in citrate buffer with 1 μ L of H₂O₂. The colorimetric reaction was stopped by adding 50 μ L/well of 2N H₂SO₄ and the OD was measured at 492 nm in a Varioskan LUX reader (Thermo Scientific).

2.6 Statistical analysis

Unless otherwise stated, significant differences among samples were evaluated by the One-way ANOVA test using GraphPad Prism software (GraphPad software, Inc., San Diego, CA). Results shown are representative of at least three independent assays.

3 Results

3.1 PcH structural stability

The structural stability of PcH was evaluated across a wide range of temperatures and pH values by absorption and fluorescence spectroscopy. The protein showed high thermal stability, with absorption spectra showing no perturbation until 80°C (Figure 1A), where a shift to higher wavelengths in the corresponding fourth derivatives was observed (Supplementary Figure 1SA). In contrast, fluorescence spectra of PcH showed a red shift in their emission maxima as well as an increase in the spectra mass center above 60°C (Figures 1B, C), indicative of a slight structural perturbation at this temperature. Regarding pH structural stability, PcH remained stable across a range of pH from 4.0 up to 10.0, as evidenced by both absorption (Figure 1D; Supplementary Figure 1SB) and fluorescence spectroscopy (Figures 1E, F).

3.2 PcH cytotoxicity

The cell viability of THP-1 monocytes was assessed by MTT assay after exposure to different PcH concentrations, revealing a lack of cytotoxic effect after 3, 24, and 72 h of incubation (Figure 2A). The endotoxin content in hemocyanin stock preparations was undetectable in our experimental conditions.

3.3 Pro-inflammatory response

The pro-inflammatory effect of PcH on THP-1 differentiated into macrophages was confirmed by the significant increase in TNF- α and IL-1 β levels in culture supernatants in a dose-dependent manner (Figures 2B, E). This cytokine secretion pattern is consistent with a Th-1 response previously observed for other gastropod hemocyanins (12, 24). Interestingly, a significant decrease in TNF- α secretion was observed when PcH was pre-treated with sodium periodate or enzymatically de-N-glycosylated (Figures 2C, D, respectively). Regarding IL-1 β secretion pattern, a significant decrease was only observed in macrophages exposed to periodate-treated PcH (Figure 2F), while a marked, but not significant, decrease was observed for PcH enzymatically de-N-glycosylated (Figure 2G). Deglycosylation of PcH was confirmed using 6% native PAGE, which showed a shift in the electrophoretic migration pattern following both treatments (Supplementary Figure S2). These shifts are consistent with observations reported for other hemocyanins (23, 32, 37).

3.4 Monocyte differentiation

3.4.1 Morphological changes

To track the phenotypic changes during the monocyte into macrophages differentiation, the morphological changes in THP-1 human monocytes associated with PcH exposure were determined

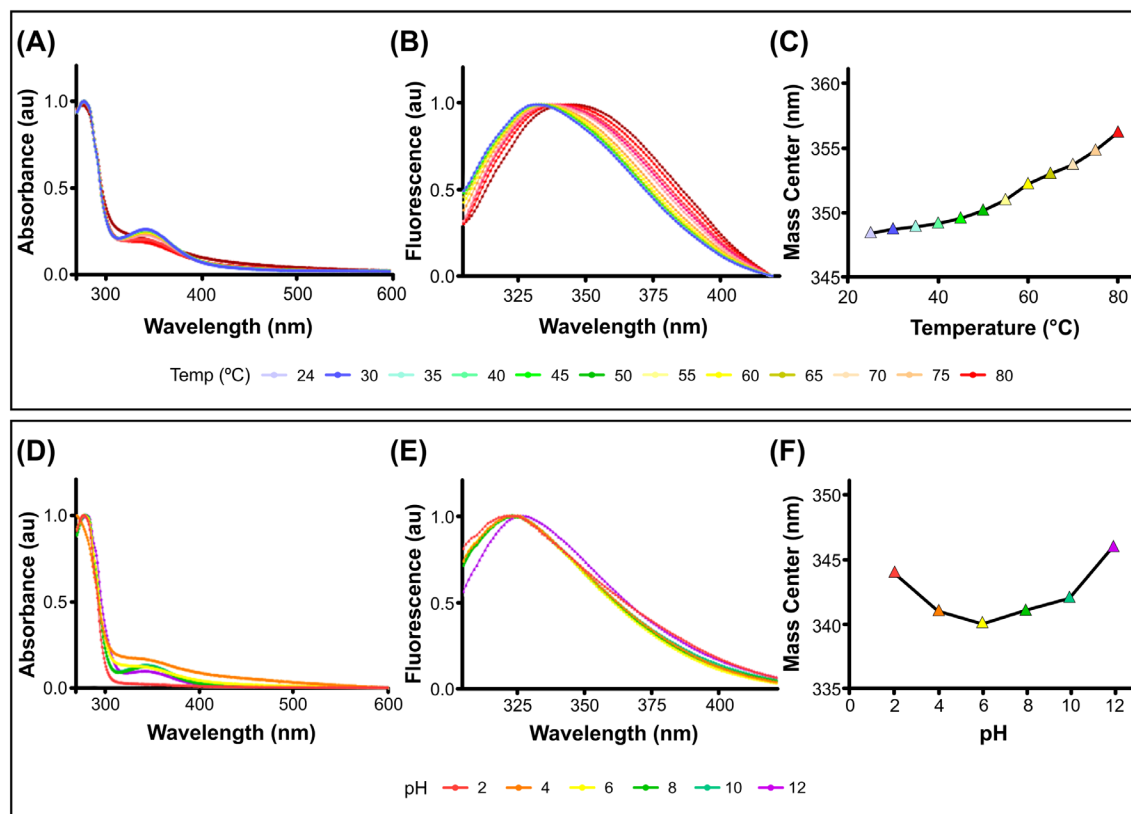


FIGURE 1

Structural stability of PcH. (A) UV-vis absorption spectra, (B) normalized intrinsic fluorescence spectra, and (C) their mass centers of PcH at different temperatures. (D) UV-Vis absorption spectra, (E) normalized intrinsic fluorescence spectra, and (F) their mass centers of PcH at different pH values.

by flow cytometry. The forward vs. side scattered light dot plots (Figure 3A) revealed the rise of a subpopulation with increased subcellular complexity and a reduction in cell size in monocytes treated with PcH compared to PBS-treated cells. These morphological changes are consistent with the effects observed with PMA treatment, which was used as a positive differentiation control.

3.4.2 Changes in cellular adhesion

Monocytes exposed to PcH underwent a phenotypic alteration from suspension-growing cells to adhered ones, as expected for THP-1 macrophage differentiation (Figure 3B). To monitor cellular behaviour, THP-1 nuclei were stained with the Hoescht-33258 dye which significantly increases its quantum yield when bound to DNA. Fluorescence microscopy observations suggested a higher number of cells adhered to the plate when treated with PcH or PMA compared to treatment with PBS alone (Figure 3C). The fluorescence quantification in each condition confirmed significant differences in the suspended/adhered cell ratio upon PcH treatment (Figure 3D).

3.4.3 Metabolic changes

Mitochondrial metabolism is highly dependent on the type of cellular differentiation that monocytes undergo. The monocyte

subpopulation with smaller size, as described above, also showed a diminished MitoTracker Deep Red fluorescence intensity (Figure 4A), suggesting that differentiating monocytes went through characteristic metabolic changes after PcH exposure. Indeed, monocytes exposed to PcH displayed a decrease in the MitoTracker MdfI compared to PBS-exposed monocytes, which is consistent with the effects observed for PMA-exposed monocytes. Such a reduction in MdfI is indicative of mitochondrial membrane hyperpolarization and a metabolic shift towards a glycolytic phenotype, as it is expected for proinflammatory M1 macrophage differentiation.

3.4.4 Macrophage differentiation markers

To confirm the macrophage differentiation of PcH-exposed monocytes, we analysed the presence of the pan-macrophage marker CD68 by Western blot. Monocyte cultures showed an increase in CD-68 for PcH and PMA-treated cells as shown in Figure 4B. To further characterize the effect of PcH on monocyte differentiation, we evaluated the differential gene expression of M1/M2 macrophage markers by qPCR. We found a significant increase in the expression levels of two M1 markers, namely CD86 and CD80, after 36 h exposure to PcH (Figure 4C). No significant changes were observed for the M2 markers employed (not shown).

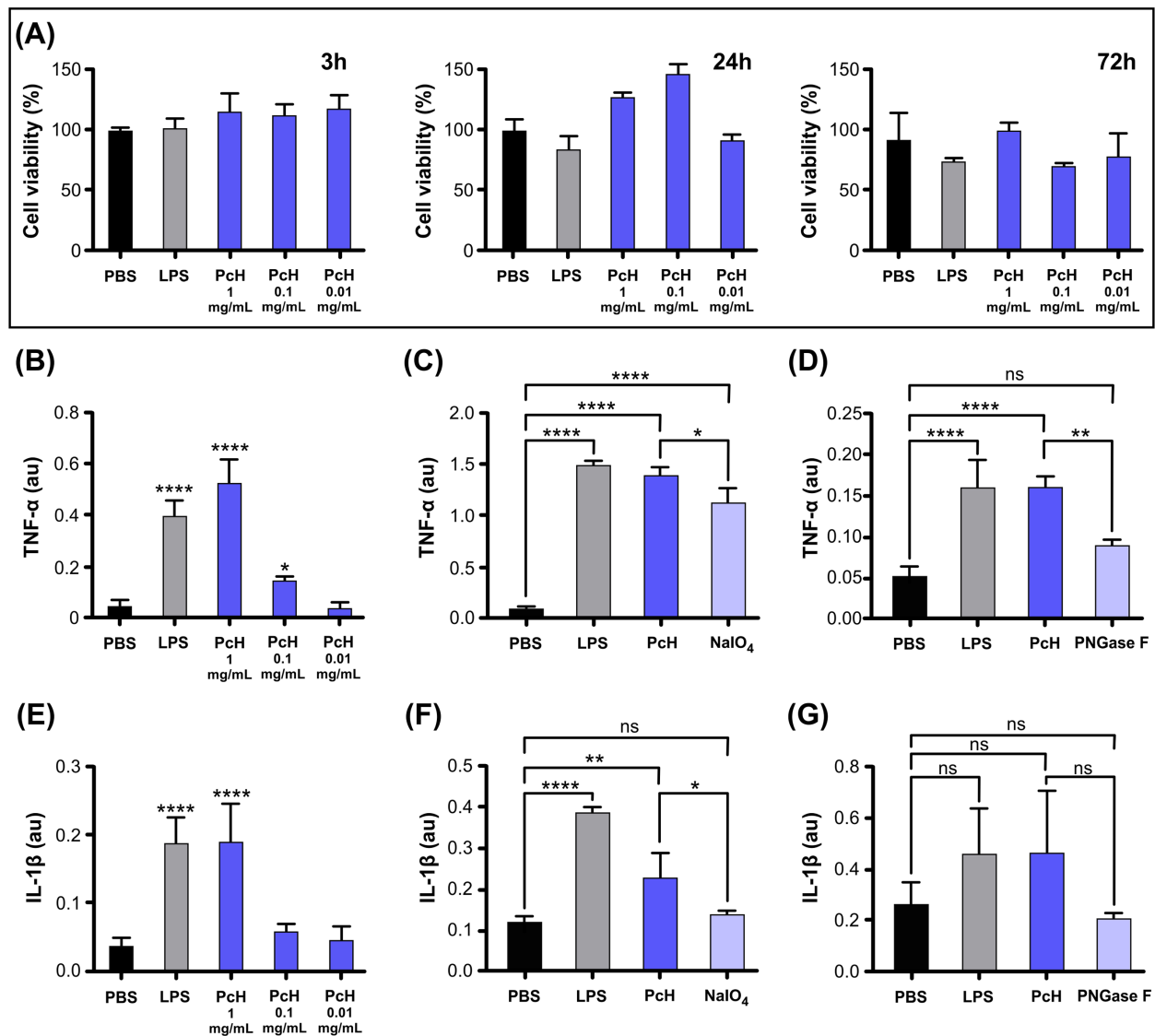


FIGURE 2

Pch cytotoxicity and induced cytokine secretion profiles on THP-1 derived macrophages. (A) Cell viability in THP-1 derived macrophages assessed by MTT assay after 3h, 24h, and 72h exposure to 1, 0.1, and 0.01 mg/mL of Pch. (B) TNF- α secretion levels induced by 1, 0.1 and 0.01 mg/mL of Pch, (C) 1 mg/mL NalO₄ oxidized Pch, and (D) 1 mg/mL de-N-glycosylated (PNGase F) Pch, after 3h exposure. (E) IL-1 β secretion levels induced by 1, 0.1 and 0.01 mg/mL of Pch, (F) 1 mg/mL NalO₄ oxidized Pch, and (G) 1 mg/mL de-N-glycosylated (PNGase F) Pch, after 3h exposure. Bars represent the mean \pm SD of 3 independent determinations, au: arbitrary units. *P<0.05; **P<0.01; ****P<1x10⁻⁴; ns, non-significant differences.

3.5 *In vivo* humoral response

The immunogenicity of Pch was evaluated *in vivo* in C57BL/6 mice. The IgG titers in the sera of Pch and KLH immunized animals were determined by ELISA, averaged and the PBS-group titer was subtracted. Notably, not-significant differences in the IgG titers between both groups of mice were observed, indicating that both, Pch and KLH trigger a similar humoral response (Figure 5).

4 Discussion

Gastropod hemocyanins have rapidly gained research interest due to their immunomodulatory properties, making these

glycoproteins attractive candidates for biomedical applications. Although only KLH is currently used therapeutically, a few other marine gastropod hemocyanins have shown promising results (8). No recombinant hemocyanin has been obtained, making its production entirely dependent on purification from marine snail sources. In this work, we studied the immunostimulant capacity of a freshwater gastropod hemocyanin for the first time and evaluated its structural stability across a wide range of pH and temperatures. Our results expand the knowledge on molluscan hemocyanins, providing insights into their immunogenic mechanism and potential biomedical applications.

The structural stability of Pch was evaluated in a wide range of temperature and pH values. While the protein does not completely unfold at 80°C, similar to reports for *Helix aspersa* and *H. lucorum*

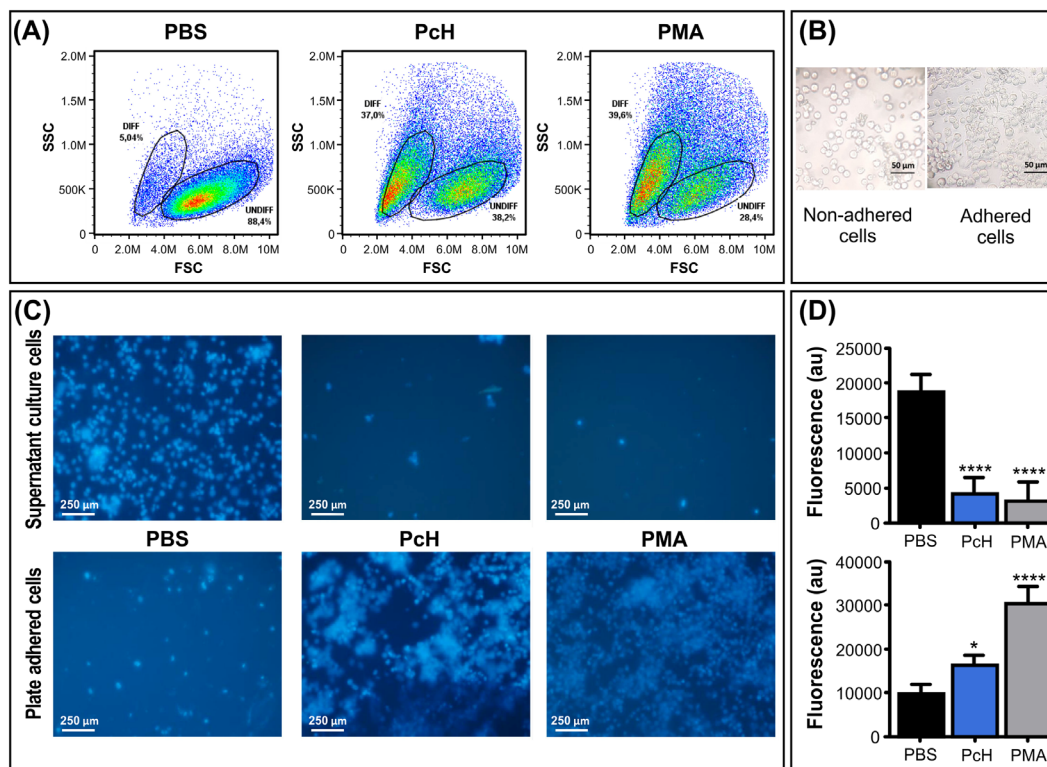


FIGURE 3

Morphological changes of monocytes upon PcH exposure. **(A)** Forward (FSC) and side light scatter (SSC) plots of THP-1 cells incubated with 1mg/mL of PcH for 72h. Gates: DIFF, differentiated monocytes; UNDIFF, undifferentiated monocytes. Representative data of 3 independent analyses. A total of 50,000 events per sample were acquired. PBS and 5 ng/mL of PMA were used as negative and positive controls, respectively. **(B)** Representative phase contrast photographs, and **(C)** fluorescence microscopy images of adhered and non-adhered THP-1 cells after 24h exposures to 1 mg/mL of PcH employing the nuclear-dyeing agent Hoescht-33258. **(D)** Total fluorescence intensity of the dye, au: arbitrary units. Bars represent the mean \pm SD of 3 independent determinations for each treatment. **** $P < 1 \times 10^{-4}$; * $P < 0.05$.

hemocyanins with Tm values of 79.8°C and 82.3°C, respectively (2, 4), slight structural perturbations were observed above 55°C. Interestingly, PcH remains stable across a broader range of pH values than that reported for *H. lucorum* hemocyanin (4). This structural stability of PcH in a wide range of pH and temperature values highlight the versatility of this hemocyanin as an immunostimulant molecule.

We verified the pro-inflammatory effect of PcH, through increased cytokine levels of IL1- β and TNF- α after exposing THP-1-derived macrophages to PcH. This cytokine secretion pattern is strongly associated with Th-1 response (38) and agrees with that observed for KLH (24). Previously, Yasuda and Ushio (39) found that KLH activates the inflammation-related transcription factor NF- κ B in THP-1 cells, while Zhong and collaborators (40) demonstrated that marine gastropod hemocyanins promote the differential gene expression of proinflammatory cytokines, including IL-1 β and TNF- α in murine macrophages. In this work, macrophages exposed to deglycosylated PcH (both by oxidation with sodium periodate and by PNGase F digestion) showed significantly decreased secretion levels of TNF- α . In contrast, a significant decrease in IL-1 β secretion was observed only for the periodate deglycosylated form of PcH, suggesting that carbohydrate moieties not removed by PNGase F digestion are

important players in the immunomodulatory properties of PcH. These findings are consistent with previous studies on KLH, CCH, and FLH (32, 41), highlighting the relevance of glycosylation in the immunogenic effect of molluscan hemocyanins. The high immunogenicity of native PcH may be linked to the presence of unusual glycan structures as seen in other hemocyanins (5, 15, 42–44), including the Gal β (1–6)Man unit in KLH (13) and a truncated N-glycosylation pattern in CCH (14). In particular, Gal β (1–3)GalNAc (9), an epitope cross-reactive with the Thomsen-Friedenreich (Tf) antigen [a truncated O-glycan structure that is highly overexpressed in epithelial carcinomas (45)] in KLH has been demonstrated to be immunogenic and proposed as a mediator of the beneficial effect of KLH in bladder cancer (46). Notably, the presence of Gal β (1–3) GalNAc has also been reported in PcH by lectin assays (27).

We further studied the effect of PcH on innate immunity by evaluating the phenotypic changes in THP-1 monocytes after PcH exposure. The appearance of a subpopulation with higher cellular complexity and smaller size, together with an increase in cellular adherence was observed in monocytes exposed to PcH and PMA. These phenotypic changes observed in both treatments are indicative of a monocyte-to-macrophage differentiation process

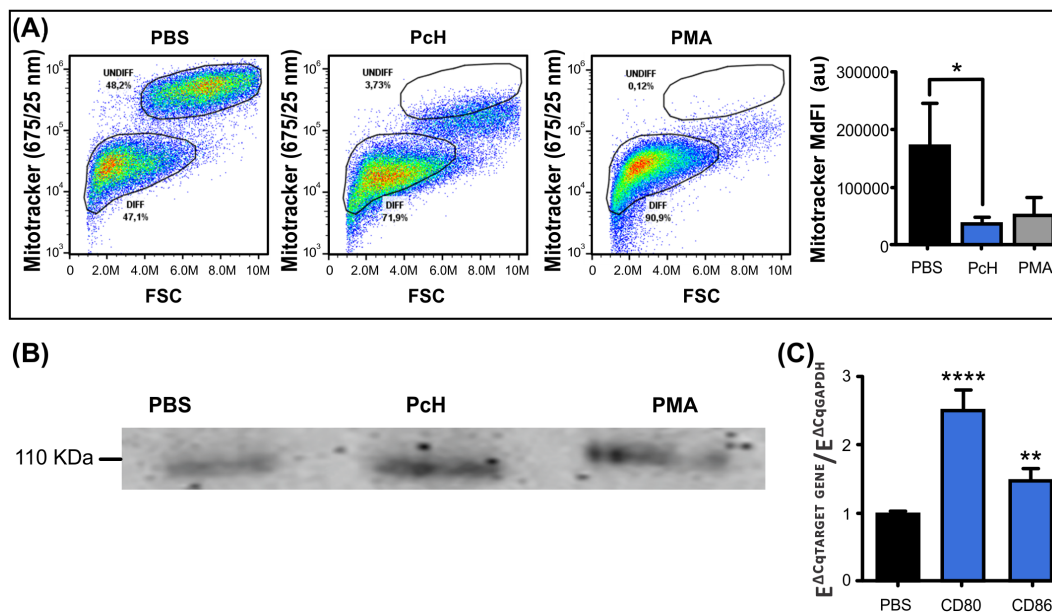


FIGURE 4

Immunometabolic changes of monocytes upon PcH exposure. **(A)** Metabolic changes on THP-1 monocytes after 1mg/mL PcH exposure as observed in MitoTracker Fluorescence vs. FSC dot plots. Gates: DIFF, differentiated monocytes; UNDIFF, undifferentiated monocytes. Median fluorescence intensity (MdfI) of the fluorescent probe were analysed by Kruskal-Wallis test, au: arbitrary units. Bars represent the mean \pm SD of 3 independent determinations for each treatment. * $P < 0.05$. A total of 50,000 events per sample were acquired. PBS and 5 ng/mL of PMA were used as negative and positive controls, respectively. **(B)** The pan macrophage marker CD68 detected by Western Blot on THP-1 cells after PcH exposure. **(C)** Differential gene expression of CD80 and CD86 M1 macrophage markers by qPCR upon PcH exposure, PBS was used as negative control. Bars represent the mean \pm SD of 3 independent determinations for each treatment. **** $P < 1 \times 10^{-4}$, ** $P < 0.01$.

(47). Moreover, a metabolic shift to a glycolytic phenotype, associated with ROS production in an M1 pro-inflammatory activation (38, 48), was also observed in monocytes exposed to PcH and PMA. The differentiation of THP-1 monocytes to macrophages was confirmed by the presence of macrophage markers in PcH-exposed monocytes, including CD68, a well-known pan macrophage marker (49, 50), and the increased differential gene expression of CD80 and CD86, indicative of M1 polarization (51). Finally, the ability to elicit a strong humoral response seems to be another key feature of the immunostimulation

induced by hemocyanins (9, 31). Native PcH was able to elicit IgG levels like those found with KLH in an *in vivo* assay, highlighting the immunogenic capability of this freshwater gastropod hemocyanin.

Based on our findings and data from other hemocyanins (9, 20, 31, 52), we propose a potential mechanism for the immunomodulatory effects of PcH. It may activate macrophages at specific sites, triggering the release of pro-inflammatory cytokines, while promoting M1 differentiation in newly recruited monocytes. This process likely involves the interaction of PcH glycan moieties with innate immune receptors, such as TLR-4 and C-type lectin (53–55), leading to a Th-1 response that helps to overcome the immune tolerance set up by tumors and other pathologies. This mechanism aligns with the complex structure and glycosylation pattern of PcH (27). Moreover, the very low cross-reactivity of CCH and FLH with anti-PcH polyclonal antibodies (27) suggests that PcH contains unique glycan-related epitopes with potentially different immune properties.

In this scenario, PcH emerges as a promising new immunostimulant. Derived from a well-studied freshwater gastropod, with available genomic and transcriptomic data (56, 57), PcH displays remarkable structural stability across a wide range of temperatures and pH values, expanding its potential for therapeutic applications. Given the lack of recombinant forms and the limited bioavailability of other hemocyanin sources, an easy-to-rear species with a high reproductive rate represents a promising alternative. These findings encourage further investigations into the biochemical and immunological properties of PcH, which may uncover new biomedical applications for this molluscan hemocyanin.

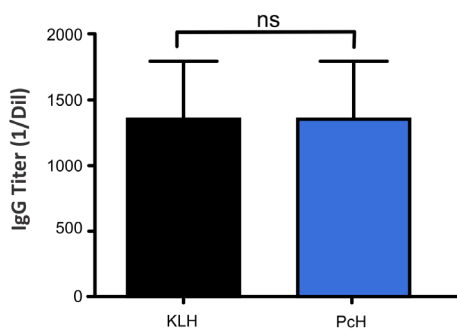


FIGURE 5

Mice humoral response to PcH. Serum IgG titers of mice immunized with PcH were compared with those immunized with KLH determined by ELISA. Bars represent the mean \pm SD of 3 independent determinations for each hemocyanin. ns, non-significant differences.

Data availability statement

The original contributions presented in the study are included in the article/**Supplementary Material**. Further inquiries can be directed to the corresponding author.

Ethics statement

Ethical approval was not required for the studies on humans in accordance with the local legislation and institutional requirements because only commercially available established cell lines were used. The animal study was approved by Comité Institucional de Cuidado y Uso de Animales de Experimentación (CICUAL) of the School of Medicine, UNLP. Protocol Number: P02-01-2024. The study was conducted in accordance with the local legislation and institutional requirements.

Author contributions

IC: Writing – original draft, Conceptualization, Data curation, Formal analysis, Investigation, Methodology, Software. MT: Writing – original draft, Conceptualization, Data curation, Formal analysis, Investigation, Methodology, Resources. MFC: Writing – original draft, Conceptualization, Investigation, Methodology. SI: Writing – original draft, Conceptualization, Data curation, Formal analysis, Investigation, Methodology. JT: Writing – original draft, Conceptualization, Formal analysis, Investigation, Methodology. KM: Writing – original draft, Conceptualization, Data curation, Formal analysis, Investigation, Resources. PS: Writing – original draft, Conceptualization, Data curation, Formal analysis, Investigation, Methodology, Resources. HH: Writing – original draft, Conceptualization, Formal analysis, Funding acquisition, Investigation, Resources. MD: Writing – original draft, Conceptualization, Data curation, Formal analysis, Funding acquisition, Investigation, Methodology, Project administration, Resources, Software, Supervision, Validation, Visualization.

Funding

The author(s) declare financial support was received for the research, authorship, and/or publication of this article. This work

References

- Ji R, Guan L, Hu Z, Cheng Y, Cai M, Zhao G, et al. A comprehensive review on hemocyanin from marine products: Structure, functions, its implications for the food industry and beyond. *Int J Biol Macromol.* (2024) 269:132041. doi: 10.1016/j.ijbiomac.2024.132041
- Todinova S, Raynova Y, Idakieva K. Irreversible thermal denaturation of Helix aspersa maxima hemocyanin. *J Therm Anal Calorim.* (2018) 7:1–10. doi: 10.1007/s10973-018-6959-7
- Dolashki A, Velkova L, Voelter W, Dolashka P. Structural and conformational stability of hemocyanin from the garden snail *Cornu aspersum*. *Z fur Naturforsch - Sect C J Biosci.* (2019) 74:113–23. doi: 10.1515/znc-2018-0084
- Idakieva K, Todinova S, Dolashki A, Velkova L, Raynova Y, Dolashka P. Biophysical characterization of the structural stability of Helix lucorum hemocyanin. *Biotechnol Biotechnol Equip.* (2021) 35:18–28. doi: 10.1080/13102818.2020.1837010

was supported by the Agencia Nacional de Promoción de la Investigación, el Desarrollo Tecnológico y la Innovación de la República Argentina, under grant PICT 2021-00158 to MD.

Acknowledgments

MT, KM, PS, SI, and HH are researchers at CONICET, Argentina. MD is a researcher at Comisión de Investigaciones Científicas, Argentina. IC is a doctoral fellow at CONICET, Argentina. JT is a member of the CONICET support staff career. We wish to thank to Romina Becerra for her technical support in the immunoblotting assays, Gabriela Sandra Finarelli for her help in cell culture, Marianela Santana for her assistance with the qPCR assays, and Juan Manuel Lofeudo for his support in animal care and handling. We also acknowledge Mario Raúl Ramos for his contribution to figure design.

Conflict of interest

The authors declare that the research was conducted in the absence of any commercial or financial relationships that could be construed as a potential conflict of interest.

Publisher's note

All claims expressed in this article are solely those of the authors and do not necessarily represent those of their affiliated organizations, or those of the publisher, the editors and the reviewers. Any product that may be evaluated in this article, or claim that may be made by its manufacturer, is not guaranteed or endorsed by the publisher.

Supplementary material

The Supplementary Material for this article can be found online at: <https://www.frontiersin.org/articles/10.3389/fimmu.2024.1490260/full#supplementary-material>

5. Kato S, Matsui T, Gatsogiannis C, Tanaka Y. Molluscan hemocyanin: structure, evolution, and physiology. *Biophys Rev.* (2018) 10:191–202. doi: 10.1007/s12551-017-0349-4
6. Abbott M, Ustoyev Y. Cancer and the immune system: the history and background of immunotherapy. *Semin Oncol Nurs.* (2019) 35. doi: 10.1016/j.soncn.2019.08.002
7. Bergman PJ. Cancer immunotherapies. *Vet Clin North Am - Small Anim Pract.* (2019) 49:881–902. doi: 10.1016/j.cvsm.2019.04.010
8. Becker MI, Arancibia S, Salazar F, Del Campo M, De Ioannes A. Mollusk hemocyanins as natural immunostimulants in biomedical applications. In: Duc GHT, editor. *Immune Response Activation.* United Kingdom: InTech (2014). p. 45–72. doi: 10.5772/57552
9. Harris JR, Markl J. Keyhole limpet hemocyanin (KLH): a biomedical review. *Micron.* (1999) 30:597–623. doi: 10.1016/S0968-4328(99)00036-0
10. Sabbatini PJ, Ragupathi G, Hood C, Aghajanian CA, Juretzka M, Iasonos A, et al. Pilot study of a heptavalent vaccine-keyhole limpet hemocyanin conjugate plus QS21 in patients with epithelial ovarian, fallopian tube, or peritoneal cancer. *Clin Cancer Res.* (2007) 13:4170–7. doi: 10.1158/1078-0432.CCR-06-2949
11. Swaminathan A, Lucas RM, Dear K, McMichael AJ. Keyhole limpet haemocyanin - A model antigen for human immunotoxicological studies. *Br J Clin Pharmacol.* (2014) 78:1135–42. doi: 10.1111/bcp.12422
12. del Campo M, Arancibia S, Nova E, Salazar F, González A, Moltedo B, et al. Hemocianinas, una herramienta inmunológica de la biomedicina actual. *Rev Med Chil.* (2011) 139:236–46. doi: 10.1093/molbev/msz084
13. Kurokawa T, Wührer M, Lochnit G, Geyer H, Markl J, Geyer R. Hemocyanin from the keyhole limpet *Megathura crenulata* (KLH) carries a novel type of N-glycans with Gal(β1-6)Man-motifs. *Eur J Biochem.* (2002) 269:5459–73. doi: 10.1046/j.1432-1033.2002.03244.x
14. Muñoz SM, Vallejos-Baccelliere G, Manubens A, Salazar ML, Nascimento AFZ, Tapia-Reyes P, et al. Structural insights into a functional unit from an immunogenic mollusk hemocyanin. *Structure.* (2024) 32:812–823.e4. doi: 10.1016/j.str.2024.02.018
15. Staudacher E. Mollusc N-glycosylation: Structures, functions and perspectives. *Biomolecules.* (2021) 11. doi: 10.3390/biom11121820
16. Díaz-Dinamarca DA, Salazar ML, Escobar DF, Castillo BN, Valdebenito B, Díaz P, et al. Surface immunogenic protein from *Streptococcus agalactiae* and *Fissurella latimarginata* hemocyanin are TLR4 ligands and activate MyD88- and TRIF dependent signaling pathways. *Front Immunol.* (2023) 14:1186188. doi: 10.3389/fimmu.2023.1186188
17. Lamm DL, Dehaven JI, Riggs DR. Keyhole limpet hemocyanin immunotherapy of bladder cancer: Laboratory and clinical studies. *Eur Urol.* (2000) 37:41–4. doi: 10.1159/000052391
18. Idakieva K, Severov S, Svendsen I, Genov N, Stoeva S, Beltrami M, et al. Structural properties of *Rapana thomasiana* grosse hemocyanin: Isolation, characterization and N-terminal amino acid sequence of two different dissociation products. *Comp Biochem Physiol - Part B Biochem.* (1993) 106:53–9. doi: 10.1016/0305-0491(93)90006-Q
19. Tchorbanov A, Idakieva K, Mihaylova N, Doumanova L. Modulation of the immune response using *Rapana thomasiana* hemocyanin. *Int Immunopharmacol.* (2008) 8:1033–8. doi: 10.1016/j.intimp.2008.03.008
20. Stoyanova E, Mihaylova N, Ralchev N, Bradyanova S, Manoylov I, Raynova Y, et al. Immunotherapeutic potential of mollusk hemocyanins in murine model of melanoma. *Mar Drugs.* (2024) 22:220. doi: 10.3390/md22050220
21. Keller H, Lieb B, Altenhein B, Gebauer D, Richter S, Stricker S, et al. Abalone (*Haliotis tuberculata*) hemocyanin type 1 (HtH1). *Eur J Biochem.* (1999) 264:27–38. doi: 10.1046/j.1432-1327.1999.00564.x
22. Markl J, Lieb B, Gebauer W, Altenhein B, Meissner U, Harris JR. Marine tumor vaccine carriers: Structure of the molluscan hemocyanins KLH and HtH. *J Cancer Res Clin Oncol.* (2001) 127:3–9. doi: 10.1007/bf01470992
23. De Ioannes P, Moltedo B, Oliva H, Pacheco R, Faunes F, De Ioannes AE, et al. Hemocyanin of the molluscan *Concholepas concholepas* exhibits an unusual heterodecameric array of subunits. *J Biol Chem.* (2004) 279:26134–42. doi: 10.1074/jbc.M400903200
24. Moltedo B, Faunes F, Haussmann D, De Ioannes P, De Ioannes AE, Puente J, et al. Immunotherapeutic effect of concholepas hemocyanin in the murine bladder cancer model: evidence for conserved antitumor properties among hemocyanins. *J Urol.* (2006) 176:2690–5. doi: 10.1016/j.juro.2006.07.136
25. Arancibia S, Espinoza C, Salazar F, Del Campo M, Tampe R, Zhong TY, et al. A novel immunomodulatory hemocyanin from the limpet *Fissurella latimarginata* promotes potent anti-tumor activity in melanoma. *PLoS One.* (2014) 9:e87240. doi: 10.1371/journal.pone.0087240
26. Schäfer GG, Grebe LJ, Schinkel R, Lieb B. The evolution of hemocyanin genes in caenogastropoda: gene duplications and intron accumulation in highly diverse gastropods. *J Mol Evol.* (2021), 639–55. doi: 10.1007/s00239-021-10036-y
27. Chiumiento IR, Ituarte S, Sun J, Qiu JW, Heras H, Dreon MS. Hemocyanin of the caenogastropod *Pomacea canaliculata* exhibits evolutionary differences among gastropod clades. *PLoS One.* (2020) 15. doi: 10.1371/journal.pone.0228325
28. Hayes KA, Burks RL, Castro-Vazquez A, Darby PC, Heras H, Martín PR, et al. Insights from an integrated view of the biology of apple snails (caenogastropoda: Ampullariidae). *Malacologia.* (2015) 58:245–302. doi: 10.4002/040.058.0209
29. Matsukura K, Okuda M, Cazzaniga NJ, Wada T. Genetic exchange between two freshwater apple snails, *Pomacea canaliculata* and *Pomacea maculata* invading East and Southeast Asia. *Biol Invasions.* (2013) 15:2039–48. doi: 10.1007/s10530-013-0431-1
30. Guide for the care and use of laboratory animals. In: , 8th edition. The National Academy Press, Washington, D.C. p. 1–246 p. National Academies Press. Eight Edit. doi: 10.1163/1573-3912_islam_DUM_3825
31. Arancibia S, Del Campo M, Nova E, Salazar F, Becker MI. Enhanced structural stability of *Concholepas* hemocyanin increases its immunogenicity and maintains its non-specific immunostimulatory effects. *Eur J Immunol.* (2012) 42:688–99. doi: 10.1002/eji.201142011
32. Salazar ML, Jiménez JM, Villar J, Rivera M, Báez M, Manubens A, et al. N-Glycosylation of mollusk hemocyanins contributes to their structural stability and immunomodulatory properties in mammals. *J Biol Chem.* (2019) 294:19546–64. doi: 10.1074/jbc.RA119.009525
33. Karkhanis YD, Zeltner JY, Jackson JJ, Carlo DJ. A new and improved microassay to determine 2-keto-3-deoxyoctonate in lipopolysaccharide of gram-negative bacteria. *Anal Biochem.* (1978) 85:595–601. doi: 10.1016/0003-2697(78)90260-9
34. Giglio ML, Ituarte S, Ibañez AE, Dreon MS, Prieto E, Fernández PE, et al. Novel role for animal innate immune molecules: enterotoxigenic activity of a snail egg MACPF-toxin. *Front Immunol.* (2020) 11:428. doi: 10.3389/fimmu.2020.00428
35. Gaddi GM, Gisonno RA, Rosù SA, Curto LM, Prieto ED, Schinella GR, et al. Structural analysis of a natural apolipoprotein A-I variant (L60R) associated with amyloidosis. *Arch Biochem Biophys.* (2020) 685:108347. doi: 10.1016/j.jabb.2020.108347
36. Bradford MM. A rapid and sensitive method for the quantitation of microgram quantities of protein utilizing the principle of protein-dye binding. *Anal Biochem.* (1976) 72:248–74. doi: 10.1016/0003-2697(76)90527-3
37. Raynova Y, Todinova S, Yancheva D, Guncheva M, Idakieva K. Enhanced structural stability of oxidized *Helix aspersa maxima* hemocyanin. *Curr Top Pept Protein Res.* (2019) 20:1–8.
38. Italiani P, Boraschi D. From monocytes to M1/M2 macrophages: Phenotypical vs. functional differentiation. *Front Immunol.* (2014) 5:514. doi: 10.3389/fimmu.2014.00514
39. Yasuda K, Ushio H. Keyhole limpet hemocyanin induces innate immunity via syk and erk phosphorylation. *EXCLI J.* (2016) 15:474–81. doi: 10.17179/excli2016-488
40. Palacios M, Tampe R, Del Campo M, Zhong TY, López MN, Salazar-Onfray F, et al. Antitumor activity and carrier properties of novel hemocyanins coupled to a mimotope of GD2 ganglioside. *Eur J Med Chem.* (2018) 150:74–86. doi: 10.1016/j.ejmech.2018.02.082
41. Jiménez JM, Salazar ML, Arancibia S, Villar J, Salazar F, Brown GD, et al. TLR4, but Neither Dectin-1 nor Dectin-2, Participates in the Mollusk Hemocyanin-Induced Proinflammatory Effects in Antigen-Presenting Cells From Mammals. *Front Immunol.* (2019) 10:1136. doi: 10.3389/fimmu.2019.01136
42. Wührer M, Robijn MLM, Koeleman CAM, Balog CIA, Geyer R, Deelder AM, et al. A novel Gal(β1-4)Gal(β1-4)Fuc(α1-6)-core modification attached to the proximal N-acetylglucosamine of keyhole limpet hemocyanin (KLH) N-glycans. *Biochem J.* (2004) 378:625–32. doi: 10.1042/BJ20031380
43. Becker MI, Fuentes A, Del Campo M, Manubens A, Nova E, Oliva H, et al. Immunodominant role of CCHA subunit of *Concholepas* hemocyanin is associated with unique biochemical properties. *Int Immunopharmacol.* (2009) 9:330–9. doi: 10.1016/j.intimp.2008.12.011
44. Siddiqui NI, Idakieva K, Demarsin B, Doumanova L, Compennolle F, Gielen C. Involvement of glycan chains in the antigenicity of *Rapana thomasiana* hemocyanin. *Biochem Biophys Res Commun.* (2007) 361:705–11. doi: 10.1016/j.bbrc.2007.07.098
45. Cagnoni AJ, Pérez Sáez JM, Rabinovich GA, Mariño KV. Turning-off signaling by siglecs, selectins, and galectins: Chemical inhibition of glycan-dependent interactions in cancer. *Front Oncol.* (2016) 6:109. doi: 10.3389/fonc.2016.00109
46. Wirguin I, Suturkova-Milosević L, Briani C, Latov N. Keyhole limpet hemocyanin contains Gal(β1-3)-GalNAc determinants that are cross-reactive with the T antigen. *Cancer Immunol Immunother.* (1995) 40:307–10. doi: 10.1007/BF01519630
47. Daigneault M, Preston JA, Marriott HM, Whyte MKB, Dockrell DH. The identification of markers of macrophage differentiation in PMA-stimulated THP-1 cells and monocyte-derived macrophages. *PLoS One.* (2010) 5:e8668. doi: 10.1371/journal.pone.0008668
48. Monteiro L de B, Davanzo GG, de Aguiar CF, Moraes-Vieira PMM. Using flow cytometry for mitochondrial assays. *MethodsX.* (2020) 7. doi: 10.1016/j.mex.2020.100938
49. Pulford KAF, Spos A, Cordell JL, Stross WP, Mason DY. Distribution of the CD68 macrophage/myeloid associated antigen. *Int Immunol.* (1990) 2:973–80. doi: 10.1093/intimm/2.10.973
50. Hoefert S, Hoefert CS, Albert M, Munz A, Grimm M, Northoff H, et al. Zoledronate but not denosumab suppresses macrophagic differentiation of THP-1

- cells. An aetiologic model of bisphosphonate-related osteonecrosis of the jaw (BRONJ). *Clin Oral Investig.* (2015) 19:1307–18. doi: 10.1007/s00784-014-1358-3
51. Shapouri-Moghaddam A, Mohammadian S, Vazini H, Taghadosi M, Esmaili SA, Mardani F, et al. Macrophage plasticity, polarization, and function in health and disease. *J Cell Physiol.* (2018) 233:6425–40. doi: 10.1002/jcp.26429
52. Zhong T-Y, Arancibia S, Born R, Tampe R, Villar J, Del Campo M, et al. Hemocyanins stimulate innate immunity by inducing different temporal patterns of proinflammatory cytokine expression in macrophages. *J Immunol.* (2016) 196:4650–62. doi: 10.4049/jimmunol.1501156
53. Díaz-Dinamarca DA, Salazar ML, Castillo BN, Manubens A, Vasquez AE, Salazar F, et al. Protein-based adjuvants for vaccines as immunomodulators of the innate and adaptive immune response: current knowledge, challenges, and future opportunities. *Pharmaceutics.* (2022) 14. doi: 10.3390/pharmaceutics14081671
54. Villar J, Salazar ML, Jiménez JM, Campo MD, Manubens A, Gleisner MA, et al. C-type lectin receptors MR and DC-SIGN are involved in recognition of hemocyanins, shaping their immunostimulatory effects on human dendritic cells. *Eur J Immunol.* (2021) 51:1715–31. doi: 10.1002/eji.202149225
55. Presicce P, Taddeo A, Conti A, Villa ML, Della Bella S. Keyhole limpet hemocyanin induces the activation and maturation of human dendritic cells through the involvement of mannose receptor. *Mol Immunol.* (2008) 45:1136–45. doi: 10.1016/j.molimm.2007.07.020
56. Sun J, Mu H, Ip JCH, Li R, Xu T, Accorsi A, et al. Signatures of divergence, invasiveness, and terrestrialization revealed by four apple snail genomes. *Mol Biol Evol.* (2019) 36:1507–20. doi: 10.1093/molbev/msz084
57. Ip JC, Mu H, Chen Q, Sun J, Heras H, Ituarte S, et al. AmpuBase: A transcriptomic database of eight species of apple snails (Gastropoda: Ampullariidae). *BMC Genomics.* (2018), 179. doi: 10.1186/s12864-018-4553-9